

Animal Research Paper

**Cite this article:** Afonso J, Guedes CM, Teixeira A, Santos V, Azevedo JMT, Silva SR (2019). Using real-time ultrasound for *in vivo* assessment of carcass and internal adipose depots of dairy sheep. *The Journal of Agricultural Science* **157**, 650–658. <https://doi.org/10.1017/S0021859620000106>

Received: 26 March 2019  
Revised: 7 February 2020  
Accepted: 12 February 2020


**Key words:**

Fat reserves; mature ewes; ultrasonic evaluation

**Author for correspondence:**

J. Afonso,  
E-mail: [jafonso@fmv.ulisboa.pt](mailto:jafonso@fmv.ulisboa.pt)

# Using real-time ultrasound for *in vivo* assessment of carcass and internal adipose depots of dairy sheep

J. Afonso<sup>1</sup> , C. M. Guedes<sup>2</sup>, A. Teixeira<sup>3</sup>, V. Santos<sup>2</sup>, J. M. T. Azevedo<sup>2</sup> and S. R. Silva<sup>2</sup>

<sup>1</sup>Faculdade de Medicina Veterinária, ULisboa, Avenida da Universidade Técnica 1300-477, Lisboa, Portugal; <sup>2</sup>Centro de Ciência Animal e Veterinária, Universidade de Trás-os-Montes e Alto Douro, 5001-801 Vila Real, Portugal and <sup>3</sup>CIMO, Instituto Politécnico de Bragança, 5300-253, Portugal

## Abstract

Fifty-one Churra da Terra Quente ewes (4–7 years old) were used to analyse the potential of real-time ultrasound (RTU) to predict the amount of internal adipose depots, in addition to carcass fat (CF). The prediction models were developed from live weight (LW) and RTU measurements taken at eight different locations. After correlation and multiple linear regression analysis, the prediction models were evaluated by *k*-fold cross-validation and through the ratio of prediction to deviation (RPD). All prediction models included at least one RTU measurement as an independent variable. Prediction models for the absolute weight of the different adipose depots showed higher accuracy than prediction models for fat content per kg of LW. The former showed to be very good or excellent ( $2.4 \leq \text{RPD} \leq 3.8$ ) for all adipose depots except mesenteric fat (MesF) and thoracic fat, with the model for MesF still providing useful information (RPD = 1.8). Prediction models for fat content per kg of LW were also very good or excellent for subcutaneous fat, intermuscular fat, CF and body fat ( $2.6 \leq \text{RPD} \leq 3.2$ ), while the best prediction models for omental fat, kidney knob, channel fat and internal fat still provided useful information. Despite some loss in the accuracy of the estimates obtained, there was a similar pattern in terms of RPD for models developed from LW and RTU measurements taken just at the level of the 11th thoracic vertebra. *In vivo* RTU measurements showed the potential to monitor changes in ewe internal fat reserves as well as in CF.

## Introduction

Sheep productivity and survival depend largely on the ability of the animals to retain and mobilize body fat (BF) reserves, depending on their nutritional and physiological status. In this regard, one of the most critical periods is early lactation, when the high energy demand requires the mobilization of fat reserves for milk synthesis, risking even a negative effect on postpartum ovarian activity when energy reserves are limited (Chilliard *et al.*, 1998; Butler, 2003; Friggens, 2003; Forcada and Abecia, 2006). Hence, it is important to monitor fat reserves in order to keep them at a level that does not compromise sheep productivity. Live weight (LW) and body condition score (BCS) are the most common predictors of BF reserves since they are quite simple to use and both have been considered good predictors of the level of fatness (Frutos *et al.*, 1997). In comparison with LW, BCS bypasses the effect of factors such as mature size, gut fill and physiological state (e.g. pregnancy). However, depending on the breed, there may be a different pattern of fat distribution within the body (Taylor *et al.*, 1989) and, in general, dairy breed ewes tend to deposit more fat in internal depots, while meat breed ewes tend to deposit more fat in the carcass depots (Kempster, 1981; Lambe *et al.*, 2006; Caldeira and Portugal, 2007). Given the higher proportion of non-carcass fat in the total fat of dairy breed ewes and the lower correlation between BCS and non-carcass fat than between BCS and carcass fat (CF), the accuracy of BCS as a predictor of internal fat (and total fat) can decrease (Frutos *et al.*, 1997). Therefore, there is a need for a more objective and precise method, easy to use in typical animal handling conditions, to predict the internal fat of dairy breed ewes such as Churra ewes. Several studies have already shown the high potential of ultrasonography for *in vivo* estimation of compositional traits in sheep, but most of them are concerned with lamb carcass and meat quality (Teixeira *et al.*, 2006; Ripoll *et al.*, 2009; Thériault *et al.*, 2009; Emenheiser *et al.*, 2010; Orman *et al.*, 2010; Hosseini Vardanjani *et al.*, 2014; Grill *et al.*, 2015). There have also been some studies of chemical body composition in lambs (Silva *et al.*, 2005) and mature ewes (Silva *et al.*, 2016). However, there is much less information on the use of ultrasonography for *in vivo* estimation of the internal adipose depots (IntF), namely in mature ewes. Chay-Canul *et al.* (2016) obtained poor estimates of BF reserves in Pelibuey ewes using ultrasonic measurements of

**Table 1.** Mean, standard deviation (s.d.) and ranges of live weight (LW), cold carcass weight (CW), lean, bone and adipose depots weight, and of CW and tissues expressed in terms of content per kg of LW of the ewes ( $n = 51$ )

Traits	Weight (g)			Content per kg of LW (g/kg)		
	Mean	s.d.	Range	Mean	s.d.	Range
LW	42 096	7385.6	30 857– 60 434			
CW	17 686	3726.8	11 858– 28 078	418	27.2	377–474
Lean	9454	1296.9	6787– 13 424	227	17.1	187–267
Bone	2996	390.2	2289–4238	72	11.4	49–95
SF	2942	1445.8	903–6576	67	23.9	20–116
ImF	2274	990.0	674–4378	52	15.3	17–78
CF	5219	2423.1	1577– 10 954	120	38.9	38–194
OmF	1840	969.2	152–4228	42	16.5	4.9–76
MesF	912	337.4	331–2074	21	5.7	9.3–38
ThoF	159	54.2	76–287	3.7	1.02	1.7–6.4
KKCF	1385	789.8	149–3646	31	13.4	4.8–65
IntF	4296	2037.1	736–9484	98	32.3	24–164
BF	9514	4367.7	2313– 20 438	218	68.2	74–359

SF, subcutaneous fat; ImF, intermuscular fat; CF, carcass fat; OmF, omental fat; MesF, mesenteric fat; ThoF, thoracic fat; KKCF, kidney knob and channel fat; IntF, internal fat; BF, body fat.

backfat thickness. However, working with Aragonese ewes, Mendizabal *et al.* (2003) observed that ultrasonic measurements of fat thickness at the sternum improved the estimates of BF reserves significantly when used together with LW. Silva *et al.* (2006) also obtained some promising results, testing two different probes to estimate the amount of IntF, but the experimental population included Île-de-France lambs as well as Churra da Terra Quente ewes. As in most previous studies about the use of ultrasonography to predict compositional traits, Silva *et al.* (2006) only tested a very limited number of scanning sites and the predictive value of different scanning sites can be affected by factors such as the breed or the physiological state of the experimental animals (e.g. growing animals *v.* mature animals). With this in mind, the objective of the present study was to analyse the potential of real-time ultrasound measurements (RTU) to predict carcass and the IntF of Churra da Terra Quente (CTQ) ewes, complementing the study of Silva *et al.* (2016).

## Materials and methods

### Animals, slaughter and carcass

The experimental population consisted of 51 shorn, non-pregnant and non-lactating CTQ ewes, 4–7 years old with a mean LW of  $42 \pm 7.4$  kg. Ewes were fasted for 18 h and then weighed before being stunned using a captive bolt and exsanguinated. Afterwards, the animals were skinned very carefully to minimize any removal of subcutaneous fat (SF). Once the udder and internal organs had been removed, the head was separated at the atlanto-occipital joint and the extremities separated at the level of carpal-metacarpal and tarsal-metatarsal joints (Fisher and De Boer, 1994).

### Body adipose depots

After slaughter, the IntF – mesenteric (MesF), omental (OmF), thoracic (ThoF) and kidney knob and channel fat (KKCF),

being ThoF surrounding the heart – were carefully obtained and weighed. Both MesF and OmF were removed in the research abattoir, while ThoF and KKCF were dissected later from the carcass after chilling at 4 °C for 24 h. Total weight of IntF was calculated by summing the weights of these four depots. The carcass adipose depots were obtained after full carcass dissection in muscle, bone, SF and intermuscular fat (ImF). Carcass fat was estimated as the sum of SF and ImF, and BF as the sum of IntF and CF. Table 1 shows the means, standard deviation (s.d.) and ranges for ewe traits (in absolute value and as content per kg of LW).

### Ultrasound image capture

Just before slaughter, the animals were scanned with an Aloka real-time scanner (Aloka 500 V, Tokyo, Japan) using a linear probe of 7.5 MHz (UST-5512U-7.5, Tokyo, Japan). The ewes were individually restrained in a crate to minimize movement and ensure they were standing in a similar stance. The probe was placed perpendicular to the backbone, over the 9th, 11th and 13th thoracic vertebrae, and over the 1st, 3rd and 5th lumbar vertebrae. The probe was also used at the middle of the thoracic cage, over the thoracic wall, between the 10th and 11th ribs, and over the 3rd sternbra of the sternum. At all these anatomical points, the wool was first clipped close to the skin and an ultrasound gel was used as a coupling medium. The ultrasound images were captured using a digital camera (Sony DCR-HC96E, Tokyo, Japan). During all RTU image capture sessions, the transition from one anatomical site to the other followed the same order.

### Ultrasound image analysis

The digital images recorded were examined and, once a suitable image was selected, a frame was extracted as a  $724 \times 580$  JPEG image file. The measurements were performed using Fiji software (<http://fiji.sc/Fiji>, NIH, USA). The area (MA), depth (MD) and

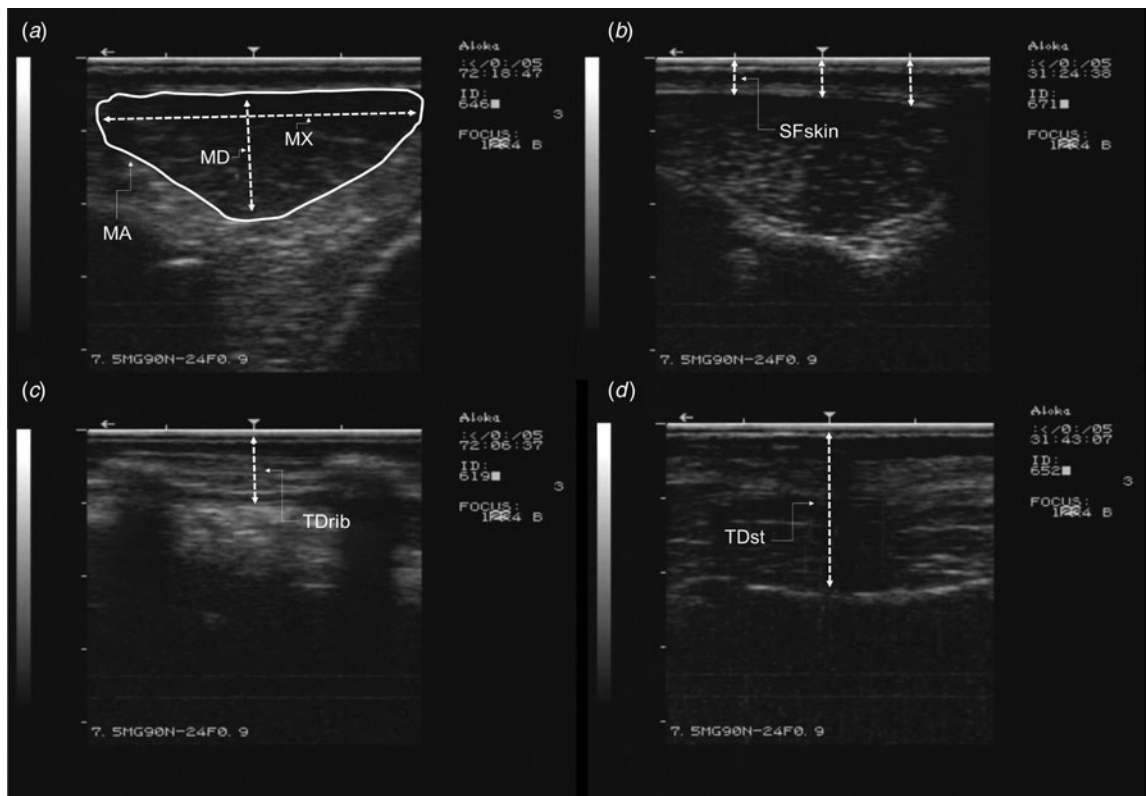


**Fig. 1.** Representative RTU images from which the measurements were taken: (a) representation of the *longissimus thoracis et lumborum* muscle measurements area (MA), depth (MD) and major axis (MX); (b) measurements of subcutaneous fat thickness plus skin were taken at three different locations to determine the mean SFSkin value. For the SF measurement, a similar procedure was followed; (c) tissue depth between the 10th and 11th ribs (TDrib) over the *obliquus externus abdominis* muscle; (d) tissue depth over the sternum (TDst).

major axis (MX) of the *longissimus thoracis et lumborum* muscle were measured in all RTU images taken over the thoracic and lumbar vertebrae, as well as SF depth with and without skin (respectively SFd and SFSkin). For all SFd and SFSkin measurements, an average of three depths was considered. This procedure allows overcoming variations in the thickness of the SF over the *longissimus thoracis et lumborum* muscle. Measurements of soft tissue depth were taken at the thoracic wall between the 10th and 11th ribs (TDrib) and over the sternum (TDst). **Figure 1** shows representative RTU images from which the measurements were taken and **Table 2** shows the means, s.d. and ranges for RTU measurements.

### Statistical analysis

A simple descriptive statistical analysis was done for LW, adipose depots and RTU measurements. The data were analysed following two different approaches – correlation analysis and multiple linear regression. The multiple regression models were built to predict the absolute weight and the content per kg of LW for carcass adipose depots, IntF and BF (dependent variables) with LW and RTU measurements (independent variables). In addition, the eight scanning sites were tested, in order to determine the single scanning site providing the most accurate estimates of all the traits of interest. These models were then combined with *k*-fold cross-validation – a tenfold cross-validation technique was used to provide an assessment of the stability of the regression models. The accuracy of the estimates was based on the *k*-fold coefficient of

determination (*k*-fold- $R^2$ ), while the root mean square error of the cross-validation (RSD<sub>cv</sub>) was used to determine the precision of the prediction model. The values of RSD<sub>cv</sub> were expressed in the same units as the dependent variable term, allowing comparison with the raw standard deviation of the variable (Lambe *et al.*, 2009). Additionally, as an indicator of the overall prediction ability of *k*-fold cross-validation models, the ratio of prediction to deviation (RPD) was evaluated, calculated as the ratio of standard deviation (s.d.) of the reference values to the RSD of cross-validation ( $RPD = s.d./RSD_{cv}$ ). All statistical procedures were carried out using the JMP software version 13 (SAS Institute, Cary, NC, USA).

### Results

**Table 3** shows the correlation values of the adipose depots (in terms of absolute weight and also in terms of content per kg of LW) with LW and the different RTU measurements. Only ThoF expressed in terms of content per kg of LW showed no significant correlation with LW ( $r = 0.174$ ;  $P > 0.05$ ) nor with RTU measurements ( $0.114 \leq r \leq 0.221$ ;  $P > 0.05$ ). All the other correlations were significant and positive. In agreement with the findings of Silva *et al.* (2006), LW and RTU measurements showed higher correlations with the different adipose depots when the latter was expressed in terms of absolute weight (g) instead of content per kg of LW. The measurements that showed the highest correlations ( $P < 0.01$ ) with the weight of most adipose depots were LW ( $0.630 \leq r \leq 0.902$ ), SFSkin ( $0.544 \leq r \leq 0.939$ ) and SFd ( $0.548 \leq r \leq$

**Table 2.** Mean (standard deviation, s.d.) and range values of real-time ultrasound (RTU) measurements obtained over the backbone, the thoracic wall and the sternum of the ewes ( $n = 51$ )

Anatomical position		RTU measurement				
		SFSkin (mm)	SFd (mm)	MD (mm)	MA (mm <sup>2</sup> )	MX (mm)
9th thoracic vertebra	Mean	8 (2.4)	6 (2.3)	18 (3.2)	600 (133.2)	41 (2.8)
	Range	4–13	2–11	13–25	374–904	36–46
11th thoracic vertebra	Mean	8 (2.4)	6 (2.5)	18 (3.2)	593 (127.9)	41 (2.9)
	Range	4–14	2–11	12–26	357–922	35–46
13th thoracic vertebra	Mean	7 (2.2)	5 (2.1)	20 (3.7)	650 (150.9)	45 (3.0)
	Range	4–12	2–9	13–27	354–965	40–51
1st lumbar vertebra	Mean	8 (2.2)	5 (2.2)	20 (3.3)	655 (141.8)	45 (3.1)
	Range	4–12	2–10	14–28	401–1002	39–51
3rd lumbar vertebra	Mean	8 (2.2)	5 (2.4)	20 (3.7)	660 (144.8)	45 (3.3)
	Range	3–13	2–10	12–28	379–1040	38–50
5th lumbar vertebra	Mean	8 (2.2)	5 (2.1)	19 (3.3)	640 (136.0)	45 (3.0)
	Range	4–12	2–9	13–27	409–997	39–50
TDrib	Mean	23 (4.1)				
	Range	14–34				
TDst	Mean	24 (5.5)				
	Range	14–34				

SFSkin, subcutaneous fat depth with skin; SFd, subcutaneous fat depth; MD, *longissimus thoracis et lumborum* muscle depth; MA, *longissimus thoracis et lumborum* muscle cross-sectional area; MX, *longissimus thoracis et lumborum* muscle major axis; TDrib, soft tissue depth at the thoracic wall between the 10th and 11th ribs; TDst, soft tissue depth at the thoracic wall over the 3rd sternbra of the sternum.

0.932). The only adipose depot with which LW and RTU muscle measurements showed higher correlations than SFSkin and SFd was MesF ( $r = 0.731$  for LW,  $0.564 \leq r \leq 0.733$  for muscle measurements and  $0.672 \leq r \leq 0.694$  for SFSkin and SFd;  $P < 0.01$ ). For SF, ImF, CF, OmF, IntF and BF expressed as content per kg of LW, there was a similar pattern regarding the RTU measurements showing the highest correlation with these adipose depots, just with smaller correlation values ( $0.788 \leq r \leq 0.929$  against  $0.849 \leq r \leq 0.939$ ;  $P < 0.01$ ). There was a larger decrease in the correlation values of LW with the different adipose depots when these were expressed as content per kg of LW than with the correlation values of the other predictors.

As shown in Table 4, across the different locations of thoracic and lumbar RTU measurements, there was a larger variation in the correlation of the different adipose depots with muscle measurements (MD, MA and MX) than with fat measurements (SFSkin and SFd). This was particularly noticeable for MD and MA – considering the correlation values of these measurements with adipose depot weights, the smallest amplitude of variation across the different thoracic and lumbar locations was observed between MA and ThoF ( $0.505 \leq r \leq 0.558$ ;  $P < 0.01$ ) and the largest was observed between MD and ImF ( $0.496 \leq r \leq 0.757$ ;  $P < 0.01$ ). Much more constant were the correlation values of SFSkin and SFd with the adipose depot weights across the different thoracic and lumbar locations, the smallest amplitude of variation being observed between SFSkin and ImF ( $0.920 \leq r \leq 0.925$ ;  $P < 0.01$ ) and the largest being observed between SFSkin and KKCF ( $0.799 \leq r \leq 0.842$ ;  $P < 0.01$ ).

All the models for the prediction of adipose depots were significant ( $P < 0.001$ ), except for ThoF expressed as content per

kg of LW ( $P = 0.081$ ), and all the models included at least one RTU measurement as an independent variable (Table 4). This shows the relevance of RTU measurements for the prediction of adipose depots, both in terms of absolute weight and as content per kg of LW. Most models included RTU measurements taken in different regions, with a larger contribution of lumbar measurements, while the measurements over the sternum (TDst) and at the thoracic wall (TDrib) showed to be less useful, but still useful to predict CF (both as a whole or separated into SF and ImF), in the case of TDst, and OmF, in the case of TDrib. The models for CF and IntF showed high accuracy, with advantage for the former (respectively  $k$ -fold- $R^2 = 0.938$  and  $0.868$ , for absolute weight, and  $k$ -fold- $R^2 = 0.904$  and  $0.718$ , for content per kg of LW). As could be expected from the correlation analysis, the highest accuracies of the models for the prediction of each adipose depot were obtained when the dependent variable was expressed in terms of absolute weight. This was particularly evident for IntF but also, in a lesser degree, for ImF. The models for MesF were the only ones that did not include any measurement of fat depth, including instead several measurements of the depth and one measurement of the major axis of the *longissimus thoracis et lumborum* muscle (MX3 – major axis of the *longissimus thoracis et lumborum* muscle at the level of the 3rd lumbar vertebra). Despite these promising results, it must be recognized that models based on RTU measurements taken at eight different locations of the body are not very practical. So, Table 5 presents the best models developed from LW and RTU measurements taken just at the level of the 11th thoracic vertebra, which, considering the different adipose depots, was the location that, overall, provided the most useful measurements. As can be noted, the

**Table 3.** Correlation values between the adipose depots (weight and content per kg of LW) and LW and RTU measurements. For thoracic and lumbar RTU measurements a range of the correlation values was considered ( $n = 51$ )<sup>a</sup>

Adipose depot	Thoracic and lumbar RTU measurements							
	LW	SFSkin (mm)	SF <sub>d</sub> (mm)	MD (mm)	MA (mm <sup>2</sup> )	MX (mm)	TDrib (mm)	TDst (mm)
Weight (g)								
SF	0.874	0.928–0.938	0.914–0.932	0.561–0.777	0.744–0.810	0.759–0.791	0.764	0.844
ImF	0.889	0.920–0.925	0.906–0.919	0.496–0.757	0.705–0.785	0.756–0.784	0.744	0.846
CF	0.886	0.931–0.939	0.918–0.932	0.537–0.780	0.733–0.805	0.762–0.793	0.760	0.850
OmF	0.854	0.866–0.886	0.859–0.888	0.579–0.756	0.695–0.755	0.711–0.744	0.750	0.751
MesF	0.731	0.678–0.694	0.672–0.693	0.564–0.733	0.670–0.727	0.665–0.711	0.619	0.583
ThoF	0.630	0.544–0.586	0.548–0.580	0.342–0.501	0.505–0.558	0.495–0.503	0.481	0.451
KKCF	0.867	0.799–0.842	0.838–0.851	0.544–0.776	0.714–0.794	0.759–0.783	0.704	0.717
IntF	0.880	0.849–0.879	0.861–0.880	0.589–0.793	0.732–0.802	0.756–0.789	0.745	0.744
BF	0.902	0.912–0.928	0.911–0.928	0.573–0.800	0.748–0.821	0.776–0.808	0.769	0.819
Content per kg of LW (g/kg)								
SF	0.751	0.919–0.929	0.885–0.918	0.556–0.719	0.694–0.744	0.706–0.726	0.768	0.884
ImF	0.731	0.887–0.889	0.858–0.877	0.450–0.678	0.617–0.682	0.681–0.691	0.726	0.880
CF	0.755	0.919–0.927	0.886–0.915	0.522–0.710	0.674–0.731	0.705–0.723	0.761	0.894
OmF	0.705	0.810–0.832	0.792–0.841	0.551–0.658	0.603–0.636	0.619–0.633	0.723	0.737
MesF	0.295	0.344–0.363	0.328–0.357	0.386–0.449	0.370–0.409	0.379–0.406	0.343	0.330
ThoF	0.174	0.173–0.221	0.163–0.203	0.114–0.138	0.164–0.187	0.142–0.129	0.176	0.150
KKCF	0.745	0.742–0.796	0.789–0.802	0.522–0.710	0.649–0.717	0.711–0.717	0.689	0.712
IntF	0.727	0.788–0.828	0.795–0.832	0.570–0.714	0.648–0.701	0.683–0.697	0.722	0.735
BF	0.775	0.898–0.919	0.883–0.914	0.568–0.743	0.692–0.749	0.726–0.742	0.776	0.858

LW, live weight; RTU, real-time ultrasound; SFSkin, subcutaneous fat depth with skin; SF<sub>d</sub>, subcutaneous fat depth; MD, *longissimus thoracis et lumborum* muscle depth; MA, *longissimus thoracis et lumborum* muscle cross-sectional area; MX, *longissimus thoracis et lumborum* muscle major axis; TDrib, soft tissue depth at the thoracic wall between the 10th and 11th ribs; TDst, soft tissue depth at the thoracic wall over the 3rd sternebra of the sternum; SF, subcutaneous fat; ImF, intermuscular fat; CF, carcass fat; OmF, omental fat; MesF, mesenteric fat; ThoF, thoracic fat; KKCF, kidney knob and channel fat; IntF, internal fat; BF, body fat.

<sup>a</sup> $r < 0.272$ ,  $P > 0.05$ ;  $r > 0.273$ ,  $P < 0.05$ ;  $r > 0.354$ ,  $P < 0.01$ .

models using RTU measurements taken just at the level of the 11th thoracic vertebra provided more accurate estimates of adipose depot weights than that of adipose depot content per kg of LW. It is the same pattern already observed with the models developed using RTU measurements taken at all the locations tested (Table 4). However, there was a significant reduction in accuracy, of between 1.3% for BF and 21.4% for MesF, for the estimates of adipose content per kg of LW, in comparison with the estimates for adipose tissue weights. Nevertheless, excluding ThoF weight estimates, which always showed low accuracy (Tables 4 and 5), MesF weight was the only trait for which the best model developed from RTU measurements taken just at the level of the 11th thoracic vertebra showed moderate accuracy ( $k$ -fold- $R^2 = 0.579$ ;  $P < 0.001$ ; Table 5), while the best model developed from RTU measurements taken at all the locations tested showed high accuracy ( $k$ -fold- $R^2 = 0.737$ ;  $P < 0.001$ ; Table 4). For all the other adipose depot weights, the best models showed high accuracy, regardless of having been developed using RTU measurements taken at all the locations tested ( $0.842 \leq k$ -fold- $R^2 \leq 0.938$ ;  $P < 0.001$ ; Table 4) or taken just at the level of the 11th thoracic vertebra ( $0.774 \leq k$ -fold- $R^2 \leq 0.920$ ;  $P < 0.001$ ; Table 5).

## Discussion

Live weight is an easy trait to obtain and, therefore, it is generally accepted as a useful predictor of body composition in general and BF in particular. The present study confirms the usefulness of LW as a predictor of the weight of all adipose depots already noted, for instance, by Mendizabal *et al.* (2003) for Aragonese ewes. In fact, the correlations of SF, ImF, OmF and KKCF with LW, obtained by Mendizabal *et al.* (2003), were very close to the corresponding values in the current work. The inclusion of TDst in the models for SF and ImF is also in agreement with the results of Mendizabal *et al.* (2003), showing that fat thickness over the sternum provides much more accurate estimates for carcass adipose depots than for IntF. However, the present results show SF depths (with or without skin) as much better predictors than TDst for all adipose depots, with TDst being included only in the models for SF and ImF, while Mendizabal *et al.* (2003) showed fat thickness over the sternum as a better predictor than SF<sub>d1</sub> for all adipose depots. Working with Pelibuey ewes, Chay-Canul *et al.* (2016) showed non-significant correlations of SF<sub>d</sub> over the *longissimus thoracis et lumborum* muscle measured at two locations (between the 12th and 13th thoracic vertebrae and between the 3rd and 4th

**Table 4.** Equations (mean values  $\pm$  s.e.) and corresponding coefficient of determination  $k$ -fold ( $k$ -fold- $R^2$ ), root mean square error of the cross-validation (RSDcv) and ratio of prediction to deviation (RPD) for the prediction of adipose depots weight and adipose depots content per kg of live weight (LW) of the ewes ( $n = 51$ )

Adipose depot	Adipose depot weight (g)					Content per kg of LW (g/kg)				
	Intercept	Independent variables	$k$ -fold- $R^2$	RSDcv	RPD	Intercept	Independent variables	$k$ -fold- $R^2$	RSDcv	RPD
SF	−3565 $\pm$ 395.6	268 $\pm$ 60.0 SFSkin11	0.933	390.1	3.7	−2.1 $\pm$ 0.75	0.58 $\pm$ 0.114 SFSkin11	0.912	0.738	3.2
		2.33 $\pm$ 0.748 MA5					0.15 $\pm$ 0.038 TDst			
		49 $\pm$ 19.9 TDst					0.01 $\pm$ 0.001 MA5			
		0.04 $\pm$ 0.016 LW					−0.001 $\pm$ 0.0000 LW			
ImF	−2352 $\pm$ 284.4	0.054 $\pm$ 0.010 LW	0.923	282.5	3.5	−0.5 $\pm$ 0.40	0.37 $\pm$ 0.078 SFSkin1	0.845	0.617	2.5
		174 $\pm$ 44.0 SFSkin5					0.12 $\pm$ 0.031 TDst			
		45 $\pm$ 13.5 TDst								
CF	−6019 $\pm$ 632.6	464 $\pm$ 106.3 SFSkin1	0.938	630.3	3.8	−9 $\pm$ 3.3	0.9 $\pm$ 0.18 SFSkin1	0.904	1.244	3.1
		0.09 $\pm$ 0.026 LW					0.27 $\pm$ 0.063 TDst			
		93 $\pm$ 31.8 TDst					0.17 $\pm$ 0.083 MX5			
		3 $\pm$ 1.2 MA5								
OmF	−2104 $\pm$ 480.4	199 $\pm$ 49.3 SFD9	0.842	397.1	2.4	−0.6 $\pm$ 0.76	0.53 $\pm$ 0.088 SFD13	0.731	0.874	1.9
		0.04 $\pm$ 0.014 LW					0.09 $\pm$ 0.044 TDrib			
		41 $\pm$ 20.3 TDrib								
MesF	3288 $\pm$ 1038.5	176 $\pm$ 39.4 MD5	0.737	182.5	1.8	3 $\pm$ 2.7	0.05 $\pm$ 0.100 MD5	0.396	0.464	1.2
		−146 $\pm$ 37.1 MX3					−0.02 $\pm$ 0.069 MD9			
		−327 $\pm$ 83.4 MD9					−0.1 $\pm$ 0.12 MX3			
		303 $\pm$ 92.8 MD1					0.2 $\pm$ 0.14 MD11			
		0.02 $\pm$ 0.006 LW								
ThoF	−21 $\pm$ 37.5	0.003 $\pm$ 0.0014 LW	0.411	42.5	1.3	0.32 $\pm$ 0.048	0.2 $\pm$ 0.12 SFSkin3	0.099	0.094	1.1
		5 $\pm$ 4.7 SFSkin3					−0.2 $\pm$ 0.11 SFSkin11			
KKCF	−2166 $\pm$ 279.0	418 $\pm$ 104.1 SFSkin3	0.854	314.6	2.5	−1.4 $\pm$ 0.49	1.0 $\pm$ 0.24 SFSkin3	0.731	0.715	1.9
		0.04 $\pm$ 0.013 LW					0.003 $\pm$ 0.0011 MA5			
		−325 $\pm$ 105.9 SFSkin13					−0.7 $\pm$ 0.24 SFSkin13			
		1.6 $\pm$ 0.60 MA5								
IntF	−4811 $\pm$ 675.5	378 $\pm$ 87.8 SFSkin3	0.868	761.6	2.7	−3 $\pm$ 1.5	0.8 $\pm$ 0.15 SFSkin11	0.718	1.749	1.8
		0.09 $\pm$ 0.031 LW					0.3 $\pm$ 0.11 MD5			
		4 $\pm$ 1.5 MA5								
BF	−9972 $\pm$ 1039.7	953 $\pm$ 126.0 SFSkin11	0.932	1173.91	3.7	−7 $\pm$ 2.4	1.6 $\pm$ 0.36 SFSkin3	0.882	2.414	2.8
		0.18 $\pm$ 0.048 LW					0.4 $\pm$ 0.15 MD5			
		7 $\pm$ 2.3 MA5					0.4 $\pm$ 0.12 TDst			

SF, subcutaneous fat; ImF, intermuscular fat; CF, carcass fat; OmF, omental fat; MesF, mesenteric fat; ThoF, thoracic fat; KKCF, kidney knob and channel fat; IntF, internal fat; BF, body fat; SFSkin11 and SFSkin13, SF depth with skin at the level of the 11th and 13th thoracic vertebrae, respectively; SFSkin1, SFSkin3 and SFSkin5, SF depth with skin at the level of the 1st, 3rd and 5th lumbar vertebrae, respectively; MA5, area of the *longissimus thoracis et lumborum* muscle at the level of the 5th lumbar vertebra; TDst, soft tissue depth over the sternum; SFD9 and SFD13, SF depth at the level of the 9th and 13th thoracic vertebrae, respectively; TDrib, soft tissue depth at the thoracic wall between the 10th and 11th ribs; MD9 and MD11, depth of the *longissimus thoracis et lumborum* muscle at the level of the 9th and 11th thoracic vertebrae, respectively; MD1 and MD5, depth of the *longissimus thoracis et lumborum* muscle at the level of the 1st and 5th lumbar vertebrae, respectively; MX3 and MX5, major axis of the *longissimus thoracis et lumborum* muscle at the level of the 3rd and 5th lumbar vertebrae, respectively.

**Table 5.** Equations (mean values  $\pm$  s.e.) and corresponding coefficient of determination  $k$ -fold ( $k$ -fold- $R^2$ ), root mean square error of the cross-validation (RSDcv) and ratio of prediction to deviation (RPD), for the prediction of adipose depots weight and adipose depots content per kg of live weight (LW) of the ewes ( $n = 51$ ), based only on the RTU measurements taken at the level of the 11th vertebra

	Intercept	LW	SFSkin11	MD11	MA11	MX11	SF11	$k$ -fold- $R^2$	RSDcv	RPD
Adipose depot weight (g)										
SF	-2871 $\pm$ 470.2	0.04 $\pm$ 0.017	389 $\pm$ 45.7	-45 $\pm$ 68.0	3 $\pm$ 1.8			0.900	429.4	3.4
ImF	-1993 $\pm$ 277.6	0.05 $\pm$ 0.011	243 $\pm$ 32.7					0.865	314.4	3.2
CF	-5072 $\pm$ 613.7	0.09 $\pm$ 0.028	627 $\pm$ 73.6		2 $\pm$ 1.4			0.910	693.6	3.5
OmF	-2344 $\pm$ 385.5	0.04 $\pm$ 0.016	216 $\pm$ 43.0	34 $\pm$ 30.3				0.807	405.0	2.4
MesF	-666 $\pm$ 188.9	0.02 $\pm$ 0.007		44 $\pm$ 15.9				0.579	218.1	1.6
ThoF	-36 $\pm$ 34.9	0.004 $\pm$ 0.0008						0.359	42.5	1.3
KKCF	-2144 $\pm$ 320.8	0.06 $\pm$ 0.012	123 $\pm$ 37.7					0.774	363.4	2.2
IntF	-2594 $\pm$ 3253.3	0.11 $\pm$ 0.032	354 $\pm$ 85.2	202 $\pm$ 118.4		-108 $\pm$ 128.1		0.827	800.1	2.6
BF	-9866 $\pm$ 1085.6	0.20 $\pm$ 0.050	992 $\pm$ 130.3		5 $\pm$ 2.4			0.920	1227.1	3.6
Content per kg of LW (g/kg)										
SF	-0.8 $\pm$ 0.45		0.92 $\pm$ 0.052					0.850	8.9	2.7
ImF	-5 $\pm$ 3.2		0.2 $\pm$ 0.11		0.54 $\pm$ 0.061	-0.003 $\pm$ 0.0027		0.790	7.0	2.2
CF	-6 $\pm$ 3.6	-0.001 $\pm$ 0.0001	1.5 $\pm$ 0.15			0.2 $\pm$ 0.12		0.850	14.5	2.7
OmF	-0.5 $\pm$ 0.47		0.57 $\pm$ 0.054					0.678	9.3	1.8
MesF	0.7 $\pm$ 0.43			0.08 $\pm$ 0.023				0.077	5.2	1.1
ThoF	0.31 $\pm$ 0.048		0.01 $\pm$ 0.006					0.043	1.0	1.0
KKCF	-4 $\pm$ 2.0					0.32 $\pm$ 0.066	0.13 $\pm$ 0.056	0.637	7.8	1.7
IntF	-2 $\pm$ 1.5		0.9 $\pm$ 0.15	0.3 $\pm$ 0.12				0.681	17.9	1.8
BF	-12 $\pm$ 6.3		2.3 $\pm$ 0.22			0.4 $\pm$ 0.18		0.835	26.4	2.6

SF, subcutaneous fat; ImF, intermuscular fat; CF, carcass fat; OmF, omental fat; MesF, mesenteric fat; ThoF, thoracic fat; KKCF, kidney knob and channel fat; IntF, internal fat; BF, body fat; SFSkin11, SF depth with skin at the level of the 11th thoracic vertebra; MD11, depth of the *longissimus thoracis et lumborum* muscle at the level of the 11th thoracic vertebra; MA11, area of the *longissimus thoracis et lumborum* muscle at the level of the 11th lumbar vertebra; MX11, major axis of the *longissimus thoracis et lumborum* muscle at the level of the 11th lumbar vertebra.

lumbar vertebrae) with CF ( $0.392 \leq r \leq 0.394$ ;  $P > 0.05$ ) and moderate correlations of SFd with internal fat ( $0.584 \leq r \leq 0.727$ ;  $P < 0.05$ ). Chay-Canul *et al.* (2016) concluded that the use of SFd at those two locations to predict BF reserves produced poor results and related such poor results to the relatively thin SF cover of the Pelibuey ewes. Delfa *et al.* (2000) and Teixeira *et al.* (2008) had already pointed out that, for goats, RTU fat depth measurements taken at the level of the 3rd and 4th sternbrae were the most suitable RTU measurements to assess BF composition, given that goats show lower fat deposition in the lumbar region and a considerably thicker amount of SF in the sternal region. Although Delfa *et al.* (2000) and Teixeira *et al.* (2008) worked with goats rather than ewes, their results support the idea presented by Chay-Canul *et al.* (2016) that, depending on the differences in fat partitioning and/or distribution between different sheep breeds, the RTU measurements included in the prediction models of BF composition may be different for different breeds. Less clear is the reason for the difference between the results of the present study and those of Mendizabal *et al.* (2003), concerning the relative importance of TDst and SFd1 as the predictors of the different adipose depots. In fact, there was no significant difference in the mean value of SFd1 in the two studies and, despite a trend for a smaller TDst in the present

study, the difference observed did not reach a significant level. Gomes *et al.* (2012) showed moderate correlations of SFd over the *longissimus thoracis et lumborum* muscle, measured 24 h post-mortem at the 12th–13th rib region, with OmF and total visceral fat ( $r = 0.43$ ;  $P < 0.01$ ), and non-significant correlations of the same SFd measurement with pelvic and heart fat, and MesF, working with crossbred sheep (Texel-cross or Santa Ines-cross). The results of Gomes *et al.* (2012) are not in line with the present results and those of Mendizabal *et al.* (2003). However, it must be pointed out that most of the animals used by Gomes *et al.* (2012) were lambs and this could justify the lower correlations obtained by those authors since, as already shown by Wood *et al.* (1980), different adipose depots present different growth rates. Consequently, regardless of any breed differences, the low to moderate correlations between SFd and the different IntF obtained by Gomes *et al.* (2012) are not in conflict with the present results and those of Mendizabal *et al.* (2003) for mature animals.

According to Viscarra Rossel *et al.* (2006), RPD values  $>2.5$  indicate excellent prediction models, RPD values between 2.0 and 2.5 indicate very good prediction models and RPD values between 1.8 and 2.0 indicate good prediction models still allowing quantitative predictions. Also according to the same authors, RPD

values between 1.4 and 1.8 indicate fair prediction models that can still be used for assessment, but RPD values between 1.0 and 1.4 indicate poor prediction models. Therefore, the best prediction models obtained in the present study for adipose depot weights were very good or excellent ( $2.4 \leq \text{RPD} \leq 3.8$ ) for all adipose depots except MesF (RPD = 1.8) and ThoF (RPD = 1.3), and even the model for MesF can provide useful information. The smaller RPD values of the models for MesF and ThoF can be related to the small mean weight and s.d. of these adipose depots, when compared with the other adipose depots. This became more evident when the different adipose depots were estimated in terms of content per kg of LW, thereby removing a large amount of the variation due to differences in LW, which resulted in poor RPD values of the models for MesF and ThoF. Nevertheless, the best prediction models for adipose depots expressed as content per kg of LW can be classified as very good or excellent for SF, ImF, CF and BF ( $2.6 \leq \text{RPD} \leq 3.2$ ), while the best prediction models for OmF, KKCF and IntF can provide useful information. This pattern did not change when considering only models developed from LW and RTU measurements taken just at the level of the 11th thoracic vertebra – despite some loss in the accuracy of the estimates, the best prediction models for adipose depot weights were very good or excellent ( $2.2 \leq \text{RPD} \leq 3.6$ ) for all adipose depots except MesF (RPD = 1.6) and ThoF (RPD = 1.3); and even the model for MesF can provide useful information. The best prediction models for adipose depots expressed as content per kg of LW were also very good or excellent for SF, ImF, CF and BF ( $2.2 \leq \text{RPD} \leq 2.7$ ), while the best prediction models for OmF, KKCF and IntF can still provide useful information.

Most studies concerned with the problem of meeting energy requirements of the animals, either during periods of low food availability or during periods of high energy needs (particularly at the end of gestation and early lactation), have tried to develop the methods of estimating total fat and/or energy reserves of the body. With that goal, Silva *et al.* (2016) already showed very promising results using RTU-based models, namely for animals of the same type as those used in the present study, but that approach overlooks the question of the relatively larger reserves of internal adipose tissue in dairy breeds compared to meat breeds. Mendizabal *et al.* (2007) showed that SF of adult Spanish Blanca Celtibérica goats was the depot most specialized in storing and mobilizing fat, followed by the omental depot, the perirenal depot and, finally, the mesenteric and intermuscular depots, which is consistent with the idea that the latter have a more structural function (Vernon, 1980). However, Gibb *et al.* (1992) showed that in cattle not only a dairy breed stores relatively more fat in internal depots than in SF (Wright and Russel, 1984), but also mobilize a larger proportion of fat from the internal depots, when compared to total BF mobilization, during the first 8 weeks postpartum. The present study shows the potential of *in vivo* RTU thoracic and lumbar measurements to monitor changes in internal fat and CF ewe reserves, which can provide data that can be used to improve herd management by matching physiological stages of highest energy demands with periods of high food availability. In addition, in cull ewes, the monitoring of adipose depots by *in vivo* RTU can enhance feeding strategies to improve the marketability of the carcasses. However, more studies are necessary to develop prediction models adapted to each breed type and verify the influence on the predictive value of such models of factors that, within each breed, affect milk production, such as parity (Casoli *et al.*, 1989; Kasap *et al.*, 2019), in order to obtain a better understanding of the effect of breed

differences on such models and maximize their predictive value for each breed.

**Financial support.** This research received no specific grant from any funding agency, commercial or not-for-profit sectors.

**Conflict of interest.** The authors declare there are no conflicts of interest.

**Ethical standards.** The authors declare that the care and handling of the ewes used in the present study followed the guidelines of the European Council Directive 86/609/ECC for the protection of animals used for experimental and other scientific purposes.

## References

- Butler WR (2003) Energy balance relationships with follicular development, ovulation and fertility in postpartum dairy cows. *Livestock Production Science* **83**, 211–218.
- Caldeira RM and Portugal AV (2007) Relationships of body composition and fat partition with body condition score in Serra da Estrela ewes. *Asian-Australasian Journal of Animal Science* **20**, 1108–1114.
- Casoli C, Duranti E, Morbidini L, Panella F and Vizioli V (1989) Quantitative and compositional variations of Massese sheep milk by parity and stage of lactation. *Small Ruminant Research* **2**, 47–62.
- Chay-Canul AJ, Garcia-Herrera R, Meza-Villalvazo VM, Gomez-Vazquez A, Cruz-Hernandez A, Magaña-Monforte JG and Ku-Vera JC (2016) Body fat reserves and their relationship to ultrasound back fat measurements in Pelibuey ewes. *Ecosistemas y Recursos Agropecuarios* **3**, 407–413.
- Chilliard Y, Bocquier F and Doreau M (1998) Digestive and metabolic adaptations of ruminants to undernutrition, and consequences on reproduction. *Reproduction Nutrition Development* **38**, 131–152.
- Delfa R, Teixeira A, Cadavez V, Gonzalez C and Sierra I (2000) Relationships between ultrasonic measurements in live goats and the same measurements taken on carcass. In Gruner L and Chabert Y (eds), *Proceedings of the 7th International Conference on Goats*. Paris, France: Institut de l'Élevage and INRA, pp. 833–834.
- Emenheiser JC, Greiner SP, Lewis RM and Notter DR (2010) Validation of live animal ultrasonic measurements of body composition in market lambs. *Journal of Animal Science* **88**, 2932–2939.
- Fisher AV and De Boer H (1994) The EAAP standard method of sheep carcass assessment. Carcass measurements and dissection procedures. Report of the EAAP working group on carcass evaluation, in cooperation with the CIHEAM Instituto Agronomico Mediterraneo of Zaragoza and the CEC Directorate General for Agriculture in Brussels. *Livestock Production Science* **38**, 149–159.
- Forcada F and Abecia JA (2006) The effect of nutrition on the seasonality of reproduction in ewes. *Reproduction Nutrition Development* **46**, 355–365.
- Friggins NC (2003) Body lipid reserves and the reproductive cycle: towards a better understanding. *Livestock Production Science* **83**, 219–236.
- Frutos P, Mantecón AR and Girádez FJ (1997) Relationship of body condition score and live weight with body composition in mature Churra ewes. *Animal Science* **64**, 447–452.
- Gibb MJ, Ivings WE, Dhanoa MS and Sutton JD (1992) Changes in body components of autumn-calving Holstein-Friesian cows over the first 29 weeks of lactation. *Animal Production* **55**, 339–360.
- Gomes RC, Constantino C, Fernandes F, Koritiaki NA, Niwa MVG, Marconato MN, Castro FAB and Ribeiro ELA (2012) Relationships among internal fat depots and subcutaneous fat in sheep. *Journal of Animal Science* **90**(suppl. 3), 382.
- Grill L, Ringdorfer F, Baumung R and Fuerst-Waltl B (2015) Evaluation of ultrasound scanning to predict carcass composition of Austrian meat sheep. *Small Ruminant Research* **123**, 260–268.
- Hosseini Vardanjani SM, Miraei Ashtiani SR, Pakdel A and Moradi Shahrebabak H (2014) Accuracy of real-time ultrasonography in assessing carcass traits in Torki-Ghashghaii sheep. *Journal of Agricultural Science and Technology* **16**, 791–800.



- Kasap A, Špehar M, Držaić V, Mulc D, Barać Z, Antunović Z and Mioč B** (2019) Impact of parity and litter size on dairy traits in Istrian ewes. *Journal of Central European Agriculture* **20**, 556–562.
- Kempster AJ** (1981) Fat partition and distribution in the carcasses of cattle, sheep and pigs: a review. *Meat Science* **5**, 83–98.
- Lambe NR, Conington J, McLean KA, Navajas EA, Fisher AV, Bünger L and Sustainable Livestock Systems Group, SAC** (2006) In vivo prediction of internal fat weight in Scottish Blackface lambs, using computer tomography. *Journal of Animal Breeding and Genetics* **123**, 105–113.
- Lambe NR, Navajas EA, Bünger L, Fisher AV, Roehe R and Simm G** (2009) Prediction of lamb carcass composition and meat quality using combinations of post-mortem measurements. *Meat Science* **81**, 711–719.
- Mendizabal JA, Delfa R, Arana A, Eguinoa P, González C, Treacher T and Purroy A** (2003) Estimating fat reserves in Rasa Aragonesa ewes: a comparison of different methods. *Canadian Journal of Animal Science* **83**, 695–701.
- Mendizabal JA, Delfa R, Arana A, Eguinoa P and Purroy A** (2007) Lipogenic activity in goats (Blanca Celtibérica) with different body condition scores. *Small Ruminant Research* **67**, 285–290.
- Orman A, Caliskan G and Dikmen S** (2010) The assessment of carcass traits of Awassi lambs by real-time ultrasound at different body weights and sexes. *Journal of Animal Science* **88**, 3428–3438.
- Ripoll G, Joy M, Alvarez-Rodriguez J, Sanz A and Teixeira A** (2009) Estimation of light lamb carcass composition by *in vivo* real-time ultrasonography at four anatomical locations. *Journal of Animal Science* **87**, 1455–1463.
- Silva SR, Gomes MJ, Dias-da-Silva A, Gil LF and Azevedo JM** (2005) Estimation *in vivo* of the body and carcass chemical composition of growing lambs by real-time ultrasonography. *Journal of Animal Science* **83**, 350–357.
- Silva SR, Afonso JJ, Santos VA, Monteiro A, Guedes CM, Azevedo JMT and Dias-da-Silva A** (2006) In vivo estimation of sheep carcass composition using real-time ultrasound with two probes of 5 and 7.5 MHz and image analysis. *Journal of Animal Science* **84**, 3433–3439.
- Silva SR, Afonso J, Guedes CM, Gomes MJ, Santos VA, Azevedo JMT and Dias-da-Silva A** (2016) Ewe whole body composition predicted *in vivo* by real-time ultrasonography and image analysis. *Small Ruminant Research* **136**, 173–178.
- Taylor S, Murray JI and Thonney ML** (1989) Breed and sex differences among equally mature sheep and goats. 4. Carcass muscle, fat and bone. *Animal Production* **49**, 385–409.
- Teixeira A, Matos S, Rodrigues S, Delfa R and Cadavez V** (2006) In vivo estimation of lamb carcass composition by real-time ultrasonography. *Meat Science* **74**, 289–295.
- Teixeira A, Joy M and Delfa R** (2008) In vivo estimation of goat carcass composition and body fat partition by real-time ultrasonography. *Journal of Animal Science* **86**, 2369–2376.
- Thériault M, Pomar C and Castonguay F** (2009) Accuracy of real-time ultrasound measurements of total tissue, fat, and muscle depths at different measuring sites in lamb. *Journal of Animal Science* **87**, 1801–1813.
- Vernon RG** (1980) Lipid metabolism in the adipose tissue of ruminant animals. *Progress in Lipid Research* **19**, 23–106.
- Viscarrá Rossel RA, McGlynn RN and McBratney AB** (2006) Determining the composition of mineral-organic mixes using UV-vis-NIR diffuse reflectance spectroscopy. *Geoderma* **137**, 70–82.
- Wood JD, MacFie HJH, Pomeroy RW and Twinn DJ** (1980) Carcass composition in four sheep breeds: the importance of type of breed and stage of maturity. *Animal Production* **30**, 135–152.
- Wright IA and Russel AJF** (1984) Partition of fat, body composition and body condition score in mature cows. *Animal Production* **38**, 23–32.